BLACK WIDOW OPTIMIZATION WITH DEEP ENSEMBLE VOTING CLASSIFIER FOR COLORECTAL CANCER DIAGNOSIS ON CLOUD COMPUTING ENVIRONMENT

Rajeev Kumar Tiwari[1], Dr. S. Murugappan[2]

Article History: Received: 17.09.2022 **Revised:** 02.11.2022 **Accepted:** 18.12.2022

Abstract

The emergence of Cloud Healthcare Platform for Colorectal Cancer (CC) diagnosis is crucial for effective detection and management of CC, a cancer that originates in the colon or rectum. Timely CC diagnosis considerably increases the possibilities of patient survival and successful treatment. Automated CC recognition systems are possible to enhance early analysis and treatment outcomes, decrease medical bills, and enhance access to diagnostic and screening services. Computer-aided diagnoses (CAD) system analyses clinical images like colonoscopy or CT scans, for detecting suspicious lesions, polyps, or tumors in the colon and rectum. This cloud-based healthcare platform employs advanced computer-based technology and system to facilitate accurate and early CC diagnosis through the analysis of medical images and patient information. The main objective is to improve the efficiency and reliability of CC screening, monitoring, and diagnoses. Deep learning (DL) approaches, particularly convolutional neural networks (CNNs), has shown promise in automatic CC diagnosis and are leveraged in this platform. Therefore, this study presents a new Black Widow Optimization with Deep Ensemble Voting Classifier (BWO-DEVC) technique for CC detection in the cloud platform. The objective of BWO-DEVC method is to recognize and classify the occurrence of the CC on medical images using the cloud platform. At the initial stage, the BWO-DEVC technique involves storing the medical images into the cloud environment where the execution process will be performed. In addition, the BWO-DEVC technique follows DarkNet-53 feature extractor to generate a set of feature vectors. For CC classification, the BWO-DEVC technique follows ensemble voting classifier encompassing three DL algorithms like gated recurrent unit (GRU), bidirectional LSTM (BiLSTM), and long short-term memory (LSTM). Finally, the hyperparameter selection of the DL models takes place using the BWO algorithm, which in turn enhances the CC detection results. An extensive set of experiments were made to validate the enriched CC detection results of the BWO-DEVC algorithm. The extensive outcomes highlighted that the BWO-DEVC method reaches high performance than other techniques in the CC diagnostic process.

Keywords: Computer aided diagnosis; Cloud computing; Deep learning; Colorectal cancer; Medical imaging; Black widow optimization

[1, 2]Dept. of Computer and Information Science, Annamalai University, Annamalainagar – 608 002, Tamil Nadu, India
Email: [1]rktresearchau@gmail.com, [2]drmryes@gmail.com

DOI: 10.48047/ecb/2022.11.12.162

1. Introduction

Cloud computing has drastically modified the healthcare setting, offering a numerous benefits that have transformed the way healthcare organizations operate, manage data, and deliver services. At its core, cloud computing in healthcare includes the delivery of computing resources, such as storage, processing power, and data access, over the internet [1]. This allows healthcare providers and organizations to store, access, and analyze abundance of healthcare data and applications in a scalable secure and manner. Cloud services operate on a pay-as-you-go model, reducing upfront costs and enabling organization to budget more efficiently. Also, cloud providers assume responsibility for data backups, security updates, and maintenance, relieving internal IT teams from routine operational tasks and facilitating them to focus on strategic initiatives [2]. This streamlines IT operations and improves data security and compliance, as reputable cloud vendors adhere to stringent security measures and certifications. Eventually, the flexibility and cost-effectiveness of cloud computing allow healthcare organizations to efficiently assign more resources, drive innovation, and enhance patient care delivery. Cloud computing has brought about a radical transformation in healthcare, addressing significant challenges related to data accessibility, management, cost efficiency, and scalability.

Fig. 1. Application of Cloud in Healthcare

Its impact is far-reaching, fostering collaboration, allowing data-driven insights, and finally enhancing the quality of care delivered to patients [3]. As the healthcare setting continues to embrace and evolve digital transformation, cloud computing will remain a cornerstone technology, playing a major role in shaping the future of healthcare delivery and patient outcomes. Fig. 1 shows the cloud based healthcare model.

In 2018, the worldwide tumour data proved the rate of colorectal cancer (CRC) is at its peak next to breast tumors and lung tumors. Global, it accounts for nearly 10 percent of the annual amount of tumor victims between both women and men [4]. The major dominant sufferers of this illness are persons aged 65 years old and beyond, the

danger in young victims is too important, with the maximum danger because of genetics (35%) and then other issues like overweight, smoking, and bad dietary lifestyles. These proportions indicate no tendency against failure; however, they are projected to rise by above 60 percent in the decade ahead, with above two million novel analyses and about a million demises by the following years [5]. In this context, there is a necessity to improve an ideal analysis plan for the initial and accurate recognition of CRC victims. Regular screening makes a significant stage for decrease in death rates of illness, colonoscopy (endoscopic technique) is examined as the main and direct medical analysis chosen approach for CRC. Apart from this approach, medicinal imaging methods like CT colonography, a balancing imaging technique for polyp recognition in CRC, and the histological assessment of H&E glides stay crucial method to delegate check-ups for CRC [6]. However physical remarks of these imaging conditions by specific pathologists have been chased persistently, newly, they have been demonstrated as customary and unexperienced techniques that are vastly long and labour intensive [6]. Also, inter-observer differences can be important in pathological analysis, resulting in the unfair inquiry of sorting tumors. Hence, a new consistent, and automatic method related to computer-aided diagnosis (CAD) has increased major attention and request recently [7].

Lately, different computer-assisted diagnoses (CADs) system have been presented to mechanically check for symptoms of tumor development. Artificial intelligence (AI) related therapeutic image inquiry approaches have expected the part of a choice assist apparatus because of initial analysis and help to surgeons [8]. The auto-analysis techniques are based on AI expertise like ML and DL. Like this, information inquiry assignments related to skilled awareness have later grown into expert independent and completely programmed analytic systems. Various conservative machine learning (ML) approaches are implemented to resolve medicinal difficulties and healthcare applications [9]. However, these approaches initially need feature extraction and feature selection phases, and they endure the drawbacks of not utilizing the suitable feature extraction technique and wastage of data in feature extraction. Instead, DL has developed popularity in medicinal analytic uses because of both removing these drawbacks and robust insight capability [10]. Medicinal information is typically radiographic image information, hence CNN is the famous DL framework usually employed to examine medicinal images.

This study presents a new Black Widow Optimization with Deep Ensemble Voting Classifier (BWO-DEVC) technique for CC detection in the cloud environment. The BWO-DEVC technique undergoes Gaussian filtering (GF) approach to remove the noise. In addition, the BWO-DEVC technique follows DarkNet-53 feature extractor to generate a set of feature vectors. For CC classification, the BWO-DEVC technique follows ensemble voting classifier encompassing three DL algorithms namely gated recurrent unit (GRU), bidirectional LSTM (BiLSTM), and long short term memory (LSTM). Finally, the hyperparameter selection of the DL algorithms takes place using the BWO algorithm, which in turn enhances the CC detection results. An extensive set of experiments were made to validate the enhanced CC detection results of the BWO-DEVC technique.

2. Related Works

In [11], a two-stage identification is presented for identifying CRC. In the primary phase, colonography video frames are removed and evaluated as important if they comprise a polyp, and these outcomes are then combined in the next phase in order to get a complete choice regarding the last

identification of that frame to be nonneoplastic and neoplastic. The CNN methods and modified forms of all techniques are assessed. In [12], a Metaheuristics approach with Deep CNN-based CC classification based on HI data (MDCNN-C3HI) is proposed. In the first stage, this method uses a bilateral filtering technique. Then, the model employs an improved capsule system with the Adam optimizer for the removal purpose. The method applies a DL-modified neural network classification algorithm for CRC detection. While the tunicate swarm procedure is utilized in order to modify its hyperparameters.

Zhou et al. [13] created a novel mechanism namely MCCBAM created on network attention and spatial attention tool, and then proposed a CAD approach which is dependent on CNN and MCCBAM that is termed HCCANet. In the study, HI managed with Gaussian filtering denoising and Gradient-weighted class activation map (Grad-CAM) were mainly employed to imagine RoI in HCCANet for enhancing its explainability. Narasimha Raju et al. [14] designed a novel model called Histo-CADx by employing DL approaches. The HI dataset is assumed as the input and then results acquired from the numerous CNN methods are compared. End-to-end CNN techniques are mainly employed in VGG-16, EfficientNet-B7, and DenseNet-201 experiments. Whereas the included CNN methodologies are established from a combination of end-to-end techniques.

Hossain et al. [15] main goal is to create a Computer-Aided Diagnosis (CAD) system by utilizing CNN as well as digital pathology images. The CNN framework was executed in order to classify and categorize the HI of adenocarcinomas and caring cells in the colon. This method also discovered optimization methods likely Understandable AI models, Lime, and DeepLift for understanding reason behind the ideal attained.

In [16], a collective classifier employing three different techniques namely logistic regression (LR), SVM, and RF methods is designed. The forecasts from the classifiers are combined by applying the common voting technique for creating the ensemble classifiers. Deep feature from colon and lung images are removed utilizing dual diverse systems such as LBP and VGG16. In [17], an enhanced DL technique to forecast MSI-H in CRC and then the whole slide images (WSIs) is proposed. The research added further auxiliary classifiers in order to midway layers of pre-trained methods. For predicting MSI status, a pair-wise learning method is created with the synergic system which is so-called parameter partial sharing network (PPsNet). Whereas the partial parameter is common between two DCNNs. The model is examined on a holdout as well as two external test sets.

3. The Proposed Model

In this study, we have designed an automatic cloud enabled CC detection and classification using the BWO-DEVC technique. The primary goal the BWO-DEVC method lies in the accurate recognition and classification of the CC on medical images in the cloud environment. It encompasses several sub-processes such as GF-based pre-processing, DarkNet-53 feature extractor, ensemble voting classification, and BWO-based hyperparameter tuning. Fig. 2 portrays the entire procedure of the BWO-DEVC method.

3.1. Stage I: GF-based Preprocessing

To remove the noise, the GF model is applied. GF is a generally utilized image pre-processing approach that contains executing a Gaussian blur to image [18]. This method smooths the image by decreasing high-frequency noise and sharp transitions among pixels but maintaining the entire structural features. It mechanism by convolving the image with Gaussian

kernel, but the central pixel can be allocated the maximum weight, and adjacent pixels are slowly reduced weight that relies on their distance in the central pixel.

3.2. Stage II: DarkNet-53-based Feature Extractor

The DarkNet-53 model is utilized for the extraction of the feature vectors. Here, the DarkNet-53 approach can applied for producing a feature vector. DarkNet-53 is a 53-layer DCNN to be supported as a baseline for the object recognition of YOLOv3 approach [19].

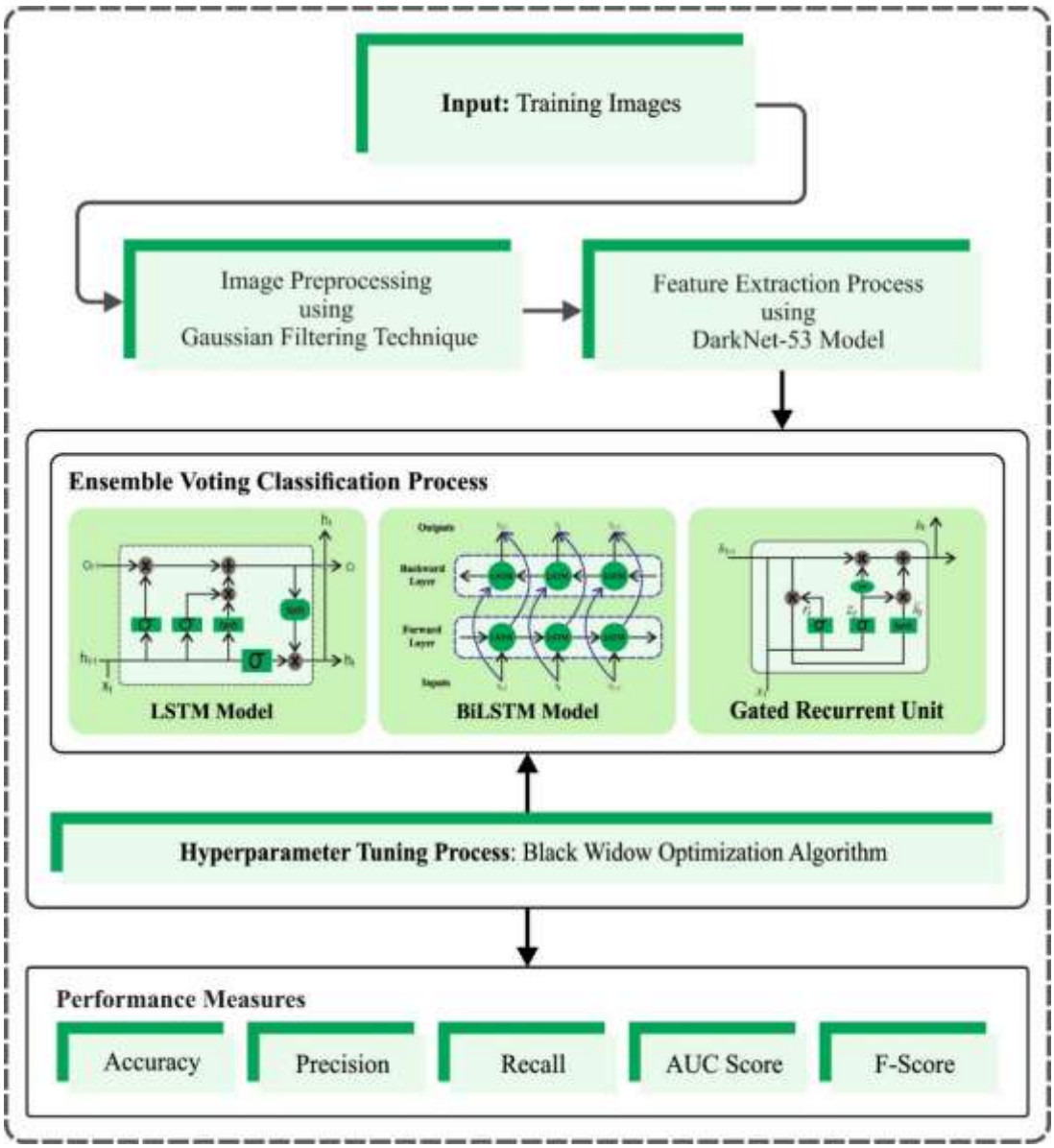

Fig. 2. Overall procedure of BWO-DEVC approach

The ResNet is combined with deep ResNet. It contains residual block and consecutive 1x1 and 3x3 Conv layers. The convolutional layer is expressed as:

$$a_m^n = \sum_{j \in X_i} a_j^{n-1} * y_{jm}^n + z_m^n \quad (1)$$

Here, $*$ exemplifies the convolution function. The input image was twisted by the convolution kernel for generating m mapping feature a_m^n , which is defined in layer n utilizing m mapping feature. The j module of m convolution kernel at layer n is represented as y_j^n. X_i illustrates the feature vectors of image.
The additional critical layer is BN layer.

$$a_{out} = \frac{\propto (a_m^n - \partial)}{\sqrt{\omega^2 + \varphi}} + \gamma \tag{2}$$

Let φ be the constant offset categorized as γ, $\propto$ which refers to the scaling factor, ∂ depicts the mean of all the outputs, and the calculation of convolutional performance is defined as a_{out}, ω implies the input variance and a_{oui} stands for the solution of BN. The outcome is normalization employing BN equivalent to the same distribution of co-efficient of the same batch of eigenvalue. Afterward, it comprises a convolutional layer that accelerates the convergence speed of network, together with avoiding over-fitting. In the next layer, the activation layer can be executed:

$$\chi_j = \begin{cases} y_j, \text{ if } a_{out} \geq 0 \\ \frac{y_j}{b_j}, \text{if } a_{oui} < 0 \end{cases} \tag{3}$$

In Eq. (3), y_j represents the input value, χ_j signifies the activation value, and b_j denotes the set parameter in $(1, +\infty)$. During this network, the maxpooling layer is employed. Afterward, all the weights are combined with 1-layer by 1D array also termed features. The feature extraction is finally considered in the resultant layer.

3.3. Stage III: Ensemble Voting Classification

In this work, the ensemble voting classifier comprising LSTM, BiLSTM, and GRU models is applied. The ensemble voting classifier for colorectal cancer detection integrates the predictions of three DL models, to collectively make more accurate and reliable diagnoses [20]. By aggregating the outputs of these diverse models, often through majority voting, the ensemble mitigates individual model biases and enhances the overall sensitivity and specificity of colorectal cancer detection. This approach harnesses the complementary strengths of various algorithms, ultimately improving diagnostic performance and aiding in early cancer identification for better patient outcomes.

Long Short-Term Memory (LSTM)

A unique structure called a memory unit or cell has been presented in LSTM. This memory unit comprises four essential elements: a neuron, forget, input, and output gates with self-recurrent structure. Through these gates, the ability of cells to access and store data for a long time. The hidden state can be computed by the LSTM model as follows:

$$i = \sigma\left(x_n U^i + s_{n-1} W^i\right) \tag{4}$$
$$f = \sigma\left(x_n U^f + s_{n-1} W^f\right) \tag{5}$$
$$O = \sigma(x_n U^o + s_{n-1} W) \tag{6}$$
$$g = \tanh(x_n U^g + s_{n-1} W^g) \tag{7}$$
$$c_n = c_{n-1} \circ f + g \circ i \tag{8}$$
$$s_n = \tanh(c_n) \circ O \tag{9}$$
$$y = \text{softmax}\,(V s_n) \tag{10}$$

RNN and FFNN are the commonly used Neural network. Intrinsically, FFNN is a kind of ANN where the output of any layer has no impact on the overall performance, viz., there is no cycle formed by the connection between them. But FFNN is processed to the network through the input and output layers.

Bidirectional LSTM

The Bi-LSTM learning algorithm is a sequential process that consists of two LSTM models namely: forward direction, and backward direction. BiLSTM efficiently rises the abundance of data accessible to the network, which gives more context. The architecture of Bi-LSTM comprises hidden, forward, and backward layers. Where x and y are the input and output, correspondingly and σ is the activation function for the layer.

Gated Recurrent Units (GRU)

Classical RNN architecture suffers from rising and vanishing gradients; this prevents the network from learning long-term dependency and makes optimization challenging. Several RNN modifications were proposed to overcome these issues, the most widespread among them is LSTM. In comparison to LSTM, GRU has improved performance, is easy to implement, and requires fewer parameters.

Where reset (α_t), update (β_t) and output (h) are gates at t time. The output of gates h_t and $\hat{h}_{t-1}$ indicates the output at t and t-1 times correspondingly, Input (X) is at t time, and the activation function ($\sigma,\ \tanh$). The weight for the input and output of models are $W_\alpha, W_\beta, W_{\hat{h}}$ and W_o. The output of training samples at t time is $\hat{y}_t$. The computation of memory cell is formulated as follows:

$$\alpha_t = \sigma\left(W_\alpha \cdot \left[\hat{h}_{t-1}, x_t\right]\right) \quad (11)$$

$$\beta_t = \sigma\left(W_\beta \cdot \left[\hat{h}_{t-1}, x_t\right]\right) \quad (12)$$

$$h_t = \tanh\left(W_{\hat{h}} \cdot \left[\alpha_t * \hat{h}_{t-1}, x_t\right]\right) \quad (13)$$

3.4. Stage IV: Hyperparameter Tuning using BWO Algorithm

In this study, the BWO algorithm optimally chooses the hyperparameters related to the DL models. The black widow spider (BWS) is a poisonous spider that originates from western Canada to southern Mexico [21]. Only female spiders (FS) are one of the poisonous types, which feed on insects like butterflies, cockroaches, and beetles. They weave webs amongst swamps, and trees and inhabit forests. Through sex pheromone, the Male spider (MS) judges the mating status of FS. MS prefers to avoid malnourished or hungry FS because FS performs cannibalism. Based on the courting strategy and sex pheromone rate of spiders, mathematical model of individual location updating is established in the traditional BWOA algorithm. The typical BWO model is discussed below.

MOVEMENT BEHAVIOR

The courtship behaviors of BWS on their weaves are modelled as spiral and linear movement behaviors, as follows:

$$X_i(t+1) = \begin{cases} \vec{x} * (t) - \vec{x}_{r_1}(t) & \text{if rand} \le 0.3 \\ \vec{x} * (t) - \cos(2\pi\beta)\vec{x}_i(t) & \text{in other case} \end{cases} \quad (14)$$

Here, the new place of i^{th} individuals, representing the movement of i^{th} spiders are $\vec{x}_i(t+1)$; a floating-point number generated randomly within $[0.4, 0.9]$ is m; the optimum search individual in the latter iteration is $\vec{x}_*(t)$; randomly generated number within [1, PopSize] is

defined as r_1; a random integer within the range of [-1.0,1.0] is represented as β; $\vec{x}_i(t)$ represents the existing search individual; Furthermore, m and β parameters allow to accomplish best exploitation and exploration during the iteration process. The size of search agent population can be described as PopSize;

PHEROMONE

During the courtship process of BWS, Pheromone plays a major role. MS would rather not be associated with cannibalism rather than search for more fertile FS to avoid the risk of mating with hungry FS. MSs are not interested in FS with low pheromone content. The pheromone content of BWS is given below:

$$pheromone(i) = f\frac{itness_{max} - fitness(i)}{ftness_{max} - fitness_{min}} \quad (15)$$

In Eq. (15), the best and worst fitness values in the existing iteration are $fitness_{max}$ and $fitness_{min}$, correspondingly; the existing fitness value of i^{th} spider is represented as $fitness(i)$.

FS with lower pheromone level represents hungry cannibals. If this FS exists, they will not be selected, but replaced by an alternative. As a result, if the pheromone value is equivalent to or lesser than 0.3, the spiders' strategy is formulated by Eq. (16).

Algorithm 1: The pseudocode of BWO

Input population size $(PopSiz)$, random initial population location, the maximum iteration number (K) and compute the fitness values and pheromone values of BW, and select the global optimum location $\vec{x}_*(t)$
For $t = l: K$
  Random initialize the parameters m, β
    For $j = 1: PopSize$
      If random < 0.3 then
        $\vec{x}_j(t+1) = \vec{x}_*(t) - m\vec{x}_{r_1}(t)$
        Else
          $\vec{x}_j(t+1) = \vec{x}_*(t) - cos(2\pi\beta)\vec{x}_j(t)$
        End if
            If Pheromone $(i) < 0.3$
          Update the BWS based on Eq. (16).
        End if
Compute the fitness of BWS $\vec{x}(t+1)$.
        If $f\left(\vec{x}_j(t+1)\right) < f\left(\vec{x}_*(t)\right)$
          $\vec{x}_*(t) = \vec{x}_j(t+1)$
        End if
      End for
Compute the pheromone of individual BWS based on Eq. (15).
End for
Output $\vec{x}_*(t)$

$$\vec{x}_i(t) = \vec{x}_*(t) + \frac{1}{2}\left[\vec{x}_{r_1}(t) - \left(-1\right)^{\sigma} * \vec{x}_{r_2}(t)\right] \quad (16)$$

Here, the new location of i^{th} spider with lower pheromone content is described as $\vec{x}_i(t)$; the optimum location of population at the last iteration is $X_*(t)$; r_1 and r_2 are randomly generated

numbers within $[1, PopSize]$, and $r_1 \neq r_{2;}\vec{x}_{r_1}(t)$ and $\vec{x}_{r_2}(t)$ characterize the $r1$ and $r2$ selected individuals correspondingly; binary random number is defined as σ $\{0,1\}$. To sum up, BWO could attain satisfactory outcomes with lower optimization parameters. Fig. 3 depicts the steps involved in BWO. The fitness optimum is a vital feature in the BWO algorithm. An encoding performance has been employed for developing the good efficiency of candidate results. Presently, the accuracy value is a primary condition deployed to design an FF.

$$Fitness = max(P) \tag{17}$$

$$P = \frac{TP}{TP + FP} \tag{18}$$

Whereas, FP and TP imply the false and true positive values.

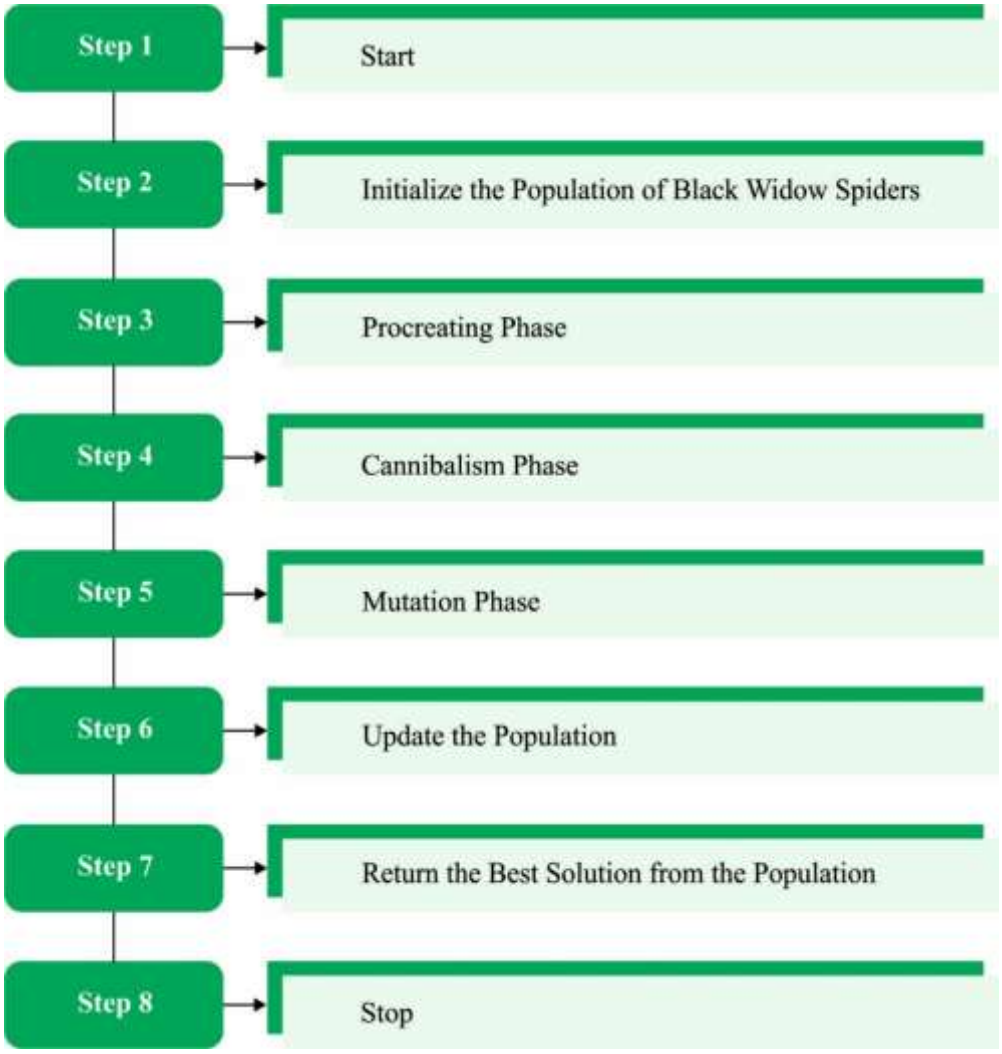

Fig. 3. Steps involved in BWO

4. Results and Discussion

The CC detection and classification performance of the BWO-DEVC technique can be validated on the Kaggle dataset [22], encompassing 10,000 samples with two classes as described in Table 1. Fig. 4 depicts the sample images.

Table 1 Details on database

Class Name	**Description**	**No. of Instances**
Col-Ad	Colon Adenocarcinoma	5000
Col-Be	Colon Benign Tissue	5000
Total Number of Instances		**10000**

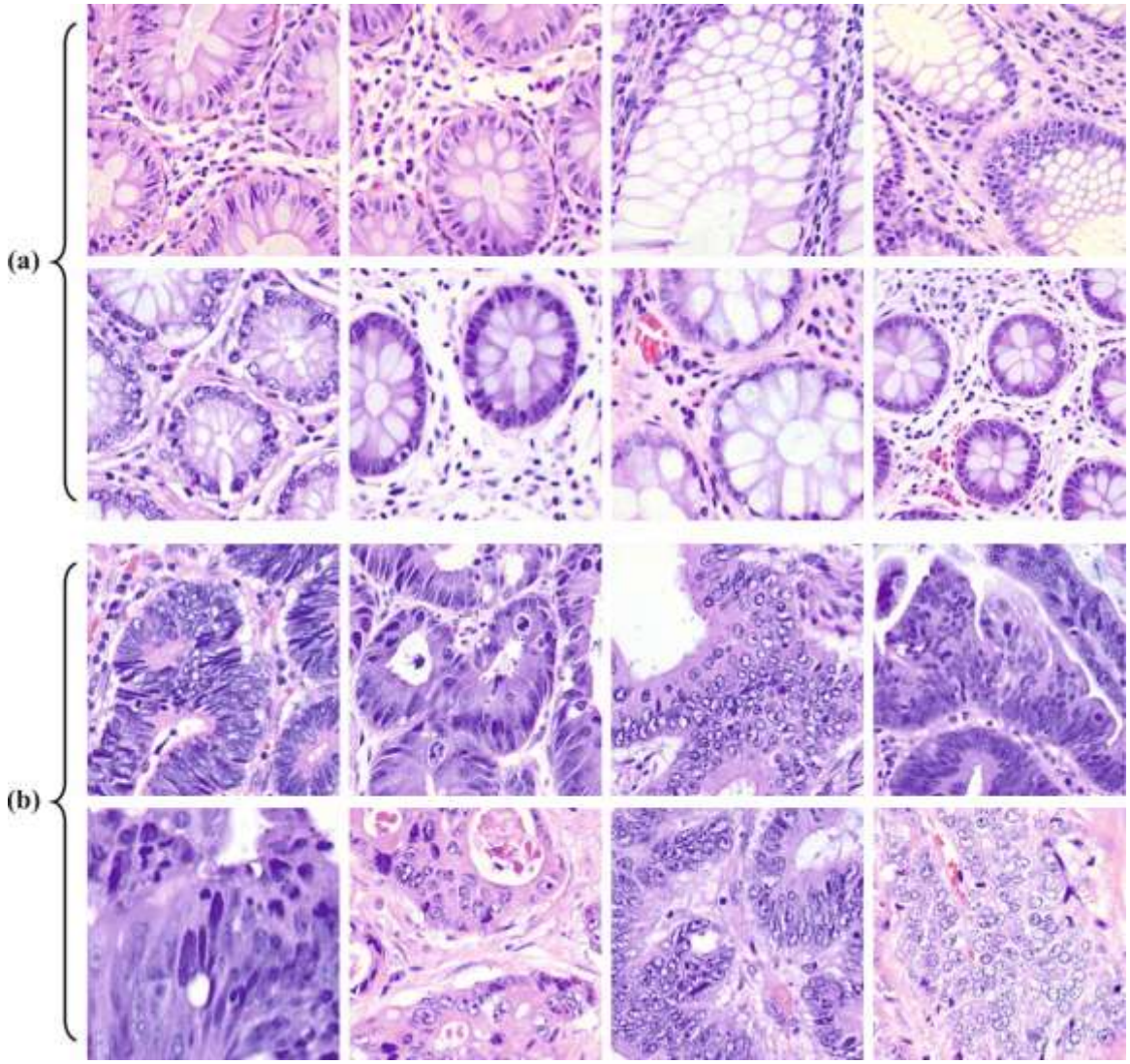

Fig. 4. Sample Images a) Colon Benign Tissue b) Colon Adenocarcinoma

Fig. 5 shows the confusion matrices produced by the BWO-DEVC technique at 80:20 and 70:30 of TR phase/TS phase. The simulated values represent the effective recognition of the Col-Ad and Col-Be samples with all two classes.

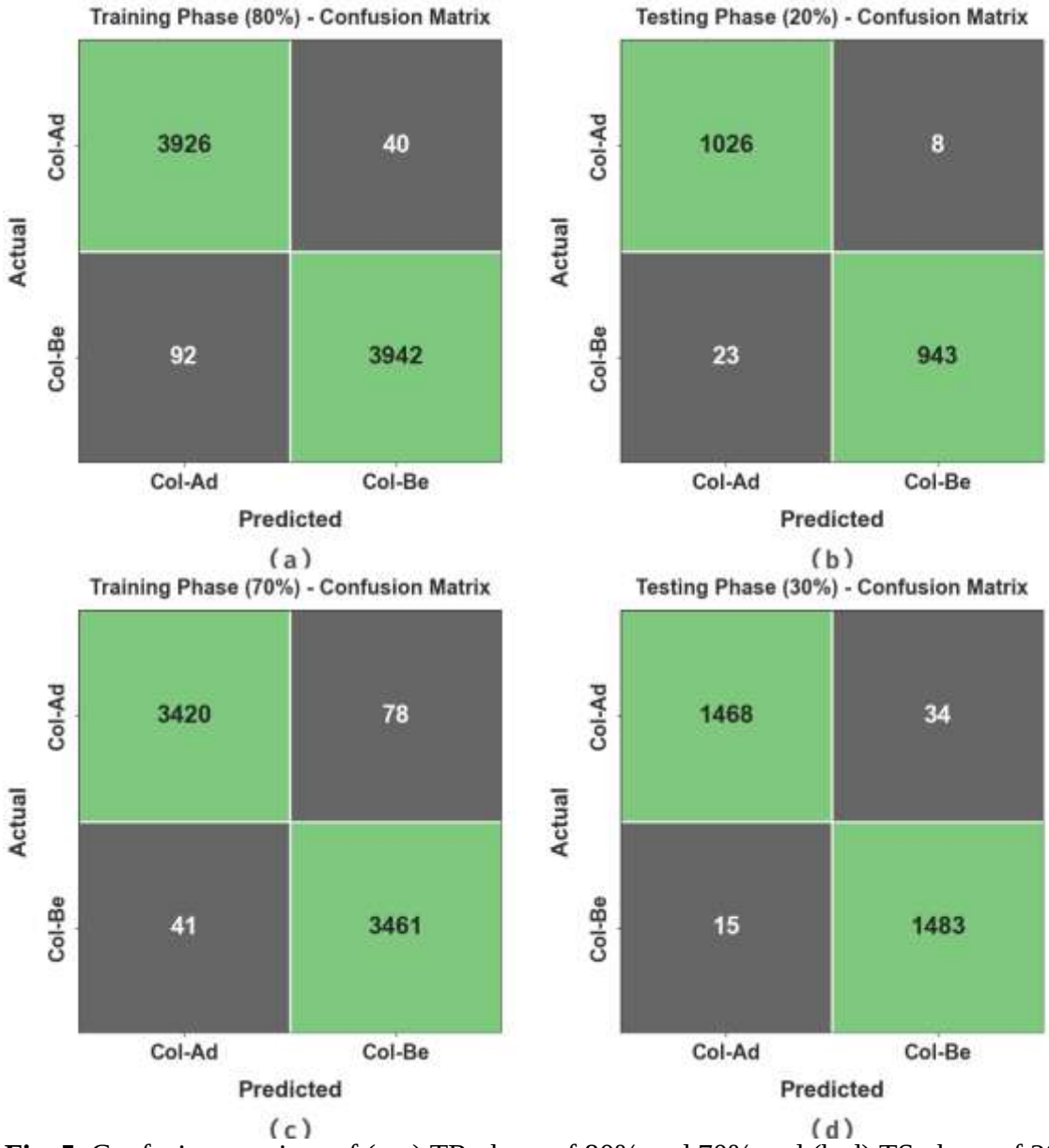

Fig. 5. Confusion matrices of (a-c) TR phase of 80% and 70% and (b-d) TS phase of 20% and 30%

The CC detection performance of the BWO-DEVC method with 80:20 of TR Phase/TS Phase is described in Table 2 and Fig. 6. The simulated values pointed out that the BWO-DEVC technique appropriately categorizes the samples. Moreover, based on 80% of TR Phase, the BWO-DEVC methodology gives average $accu_y$ of 98.36%, $prec_{\mathrm{n}}$ of 98.35%, $reca_l$ of 98.36%, F_{score} of 98.35%, and AUC_{score} of 98.36%. Also, with 20% of TS Phase, the BWO-DEVC system provides average $accu_y$ of 98.42%, $prec_n$ of 98.48%, $reca_l$ of 98.42%, F_{score} of 98.45%, and AUC_{score} of 98.42% respectively.

Table 2 CC detection outcome of BWO-DEVC algorithm on 80:20 of TR phase/TS phase

Class Labels	$\mathbf{Accu_y}$	$\mathbf{Prec_n}$	$\mathbf{Reca_l}$	$\mathbf{F_{score}}$	$\mathbf{AUC_{score}}$
TR Phase (80%)					
Col-Ad	98.99	97.71	98.99	98.35	98.36
Col-Be	97.72	99.00	97.72	98.35	98.36

Average	**98.36**	**98.35**	**98.36**	**98.35**	**98.36**
TS Phase (20%)					
Col-Ad	99.23	97.81	99.23	98.51	98.42
Col-Be	97.62	99.16	97.62	98.38	98.42
Average	**98.42**	**98.48**	**98.42**	**98.45**	**98.42**

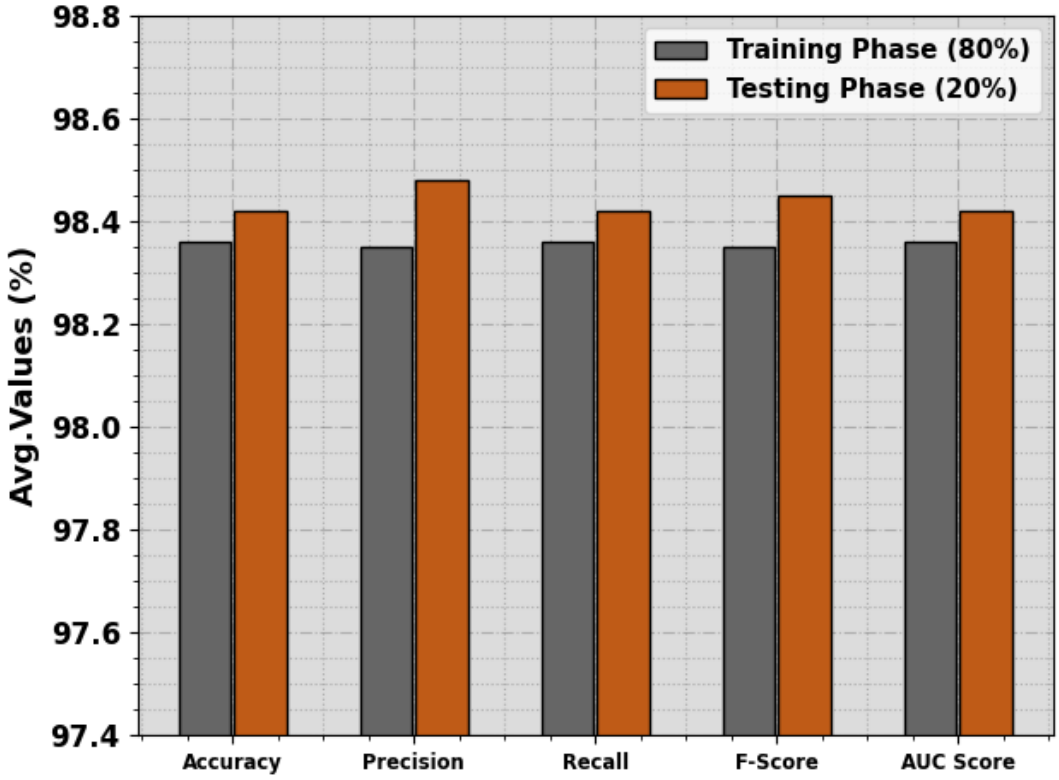

Fig. 6. Average of BWO-DEVC algorithm on 80:20 of TR phase/TS phase

The CC detection analysis of the BWO-DEVC technique with 70:30 of TR Phase/TS Phase is mentioned in Table 3 and Fig. 7. The simulated values noted that the BWO-DEVC system correctly categorizes the samples. Furthermore, based on 70% of TR Phase, the BWO-DEVC model provides average $accu_y$ of 98.30%, $prec_n$ of 98.31%, $reca_l$ of 98.30%, F_{score} of 98.30%, and AUC_{score} of 98.30%. Also, on 30% of TS Phase, the BWO-DEVC methodology gives average $accu_y$ of 98.37%, $prec_n$ of 98.37%, $reca_l$ of 98.37%, F_{score} of 98.37%, and AUC_{score} of 98.37% correspondingly.

Table 3 CC detection outcome of BWO-DEVC algorithm on 70:30 of TR phase/TS phase

Class Labels	**$Accu_y$**	**$Prec_n$**	**$Reca_l$**	**F_{score}**	**AUC_{score}**
TR Phase (70%)					
Col-Ad	97.77	98.82	97.77	98.29	98.30
Col-Be	98.83	97.80	98.83	98.31	98.30
Average	**98.30**	**98.31**	**98.30**	**98.30**	**98.30**
TS Phase (30%)					
Col-Ad	97.74	98.99	97.74	98.36	98.37
Col-Be	99.00	97.76	99.00	98.37	98.37
Average	**98.37**	**98.37**	**98.37**	**98.37**	**98.37**

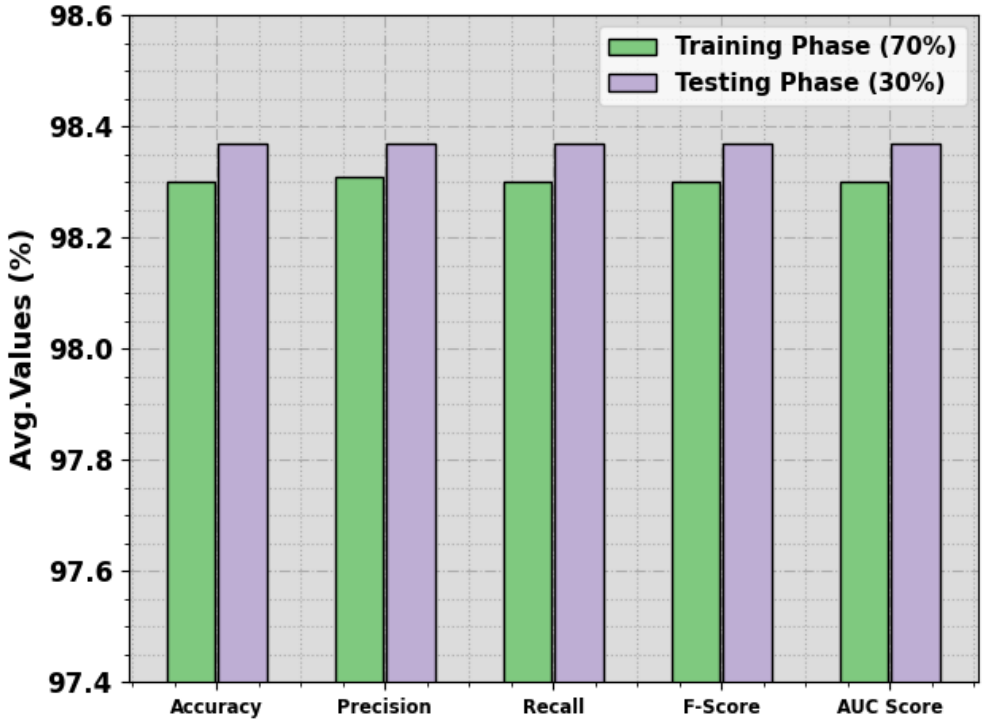

Fig. 7. Average of BWO-DEVC algorithm at 70:30 of TR phase/TS phase

To determine the performance of the BWO-DEVC method with 80:20 of TR Phase/TS Phase, TR and TS $accu_y$ curves are defined, as represented in Fig. 8. The TR and TS $accu_y$ curves show the performance of the BWO-DEVC technique over various epochs. The figure gives important details about the learning tasks and generalization abilities of the BWO-DEVC model. With a rise in epoch count, it is noticed that the TR and TS $accu_y$ curves get improved. It is observed that the BWO-DEVC system reaches enriched testing accuracy that can be potential for recognizing the patterns in the TR and TS data.

Fig. 8. $Accu_y$ curve of BWO-DEVC algorithm on 80:20 of TR phase/TS phase

Fig. 9 illustrates the overall TR and TS loss values of the BWO-DEVC methodology with 80:20 of TR Phase/TS Phase over epochs. The TR loss exhibits the model loss is diminished over epochs. Primarily, the loss values become reduced as the model adjusts the weight to decrease the predicted error on the TR and TS data. The loss curves show the extent to which the model fits the training data. It is remarked that the TR and TS loss is progressively minimized and represented that the BWO-DEVC algorithm effectively learns the patterns denoted in the TR and TS data. It is also observed that the BWO-DEVC technique vary the parameters to lessen the variance among the actual and predicted training label.

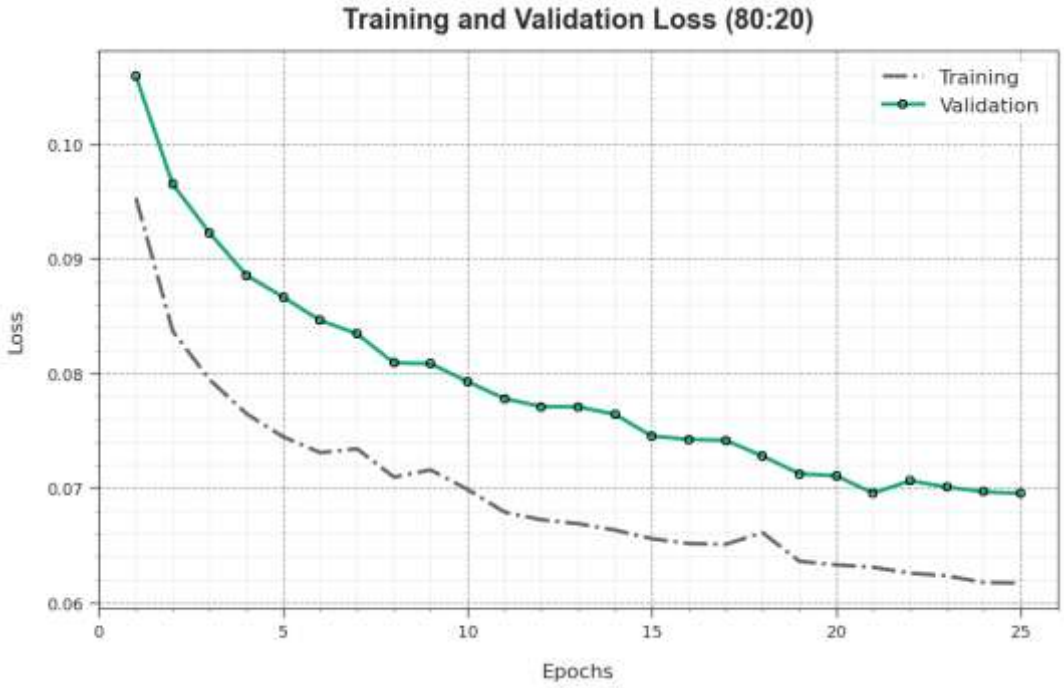

Fig. 9. Loss curve of BWO-DEVC algorithm on 80:20 of TR phase/TS phase

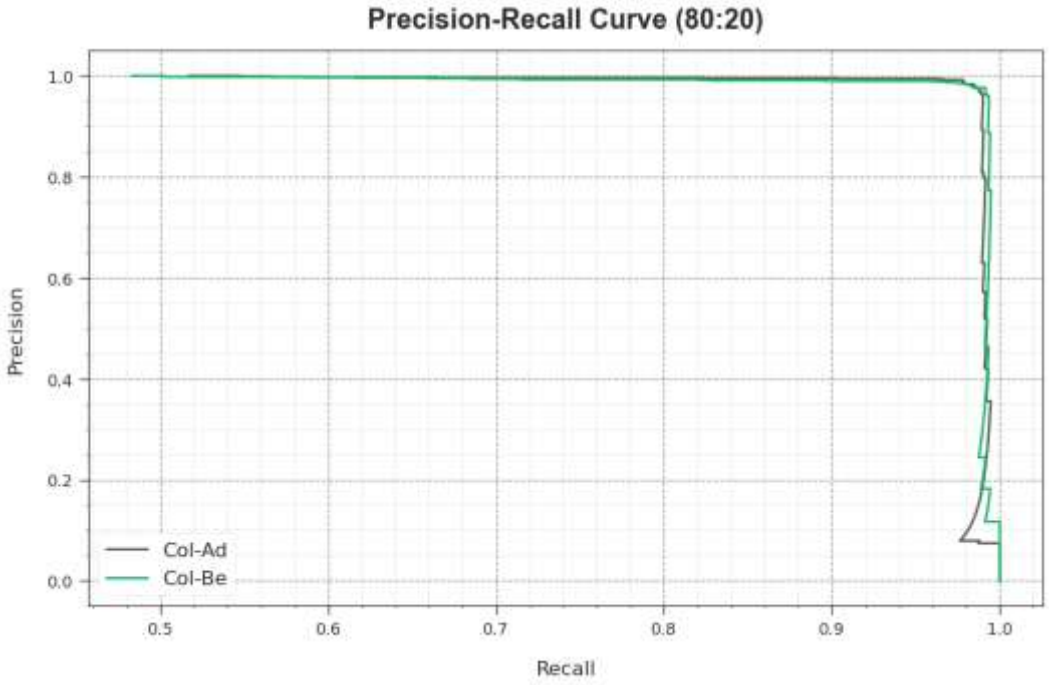

Fig. 10. PR curve of BWO-DEVC algorithm on 80:20 of TR phase/TS phase

The PR analysis of the BWO-DEVC methodology with 80:20 of TR Phase/TS Phase is illustrated by simulating precision against recall as shown in Fig. 10. The simulated values confirm that the BWO-DEVC system acquires increased PR values with each 2 class. The figure defines that the model learns to identification of diverse classes. The BWO-DEVC method attains enhanced outcomes in the recognition of positive samples with fewer false positives.

The ROC analysis offered by the BWO-DEVC system with 80:20 of TR Phase/TS Phase is represented in Fig. 11, which has the capability of the differentiation of the class labels. The figure states valuable perceptions into the trade-off among the TPR and FPR rates over diverse categorization thresholds and modifying counts of epochs. This gives the exact predicted performance of the BWO-DEVC technique on the classification of different two classes.

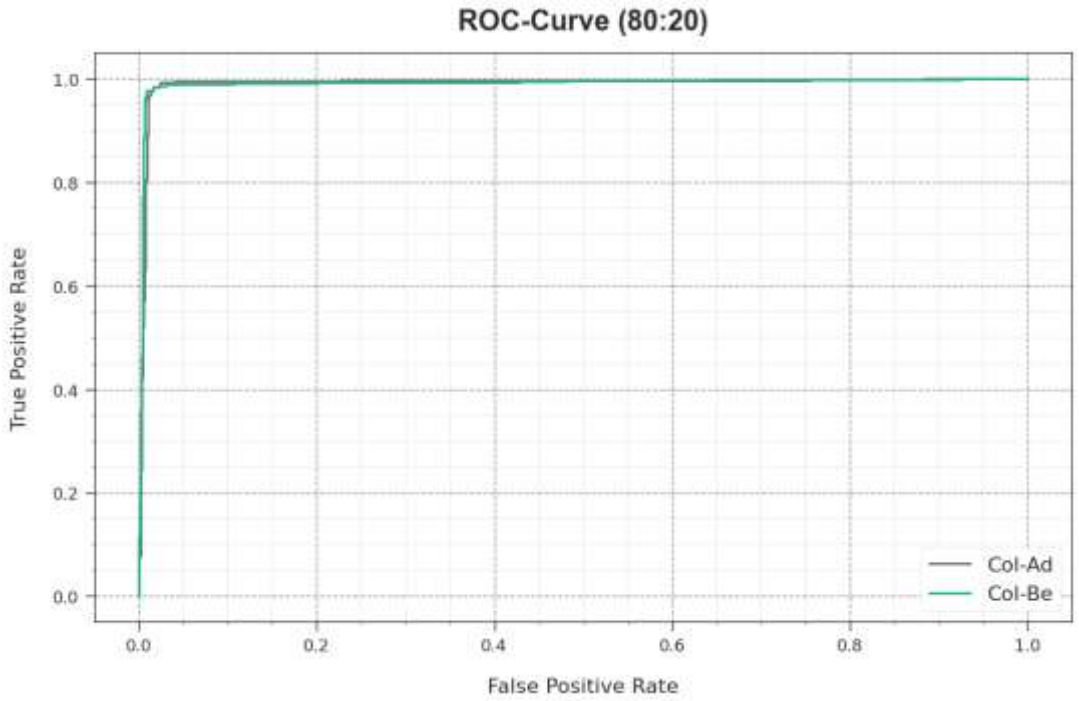

Fig. 11. ROC curve of BWO-DEVC algorithm on 80:20 of TR phase/TS phase

In Table 4 and Fig. 12, the comparative analysis of the BWO-DEVC method is clearly confirmed [12, 23, 24]. The simulated values demonstrated that the mSRC model leads to poorer performance. Simultaneously, the ResNet-50, DenseNet169-SVM, and VGG-16 methodologies exhibited moderately increased performance. Then, the CNN and DL techniques obtained remarkable performance. However, the BWO-DEVC model shows excellent performance with $accu_y$ of 98.42%, $prec_n$ of 98.48%, $reca_l$ of 98.42%, and F_{score} of 98.45%. These simulated values considered the enriched performance of the BWO-DEVC approach over other techniques.

Table 4 Comparative outcome of BWO-DEVC method with other systems

Methods	**$Accu_y$**	**$Prec_n$**	**$Reca_l$**	**F_{score}**
mSRC	88.21	85.21	91.78	86.78
RESNET-50	93.64	96.12	97.49	96.94
CNN	97.11	97.07	97.44	97.61
DL	96.32	96.86	96.44	97.08

DenseNet169 and SVM	92.08	95.82	95.67	96.15
VGG-16	91.09	95.08	96.53	97.00
BWO-DEVC	98.42	98.48	98.42	98.45

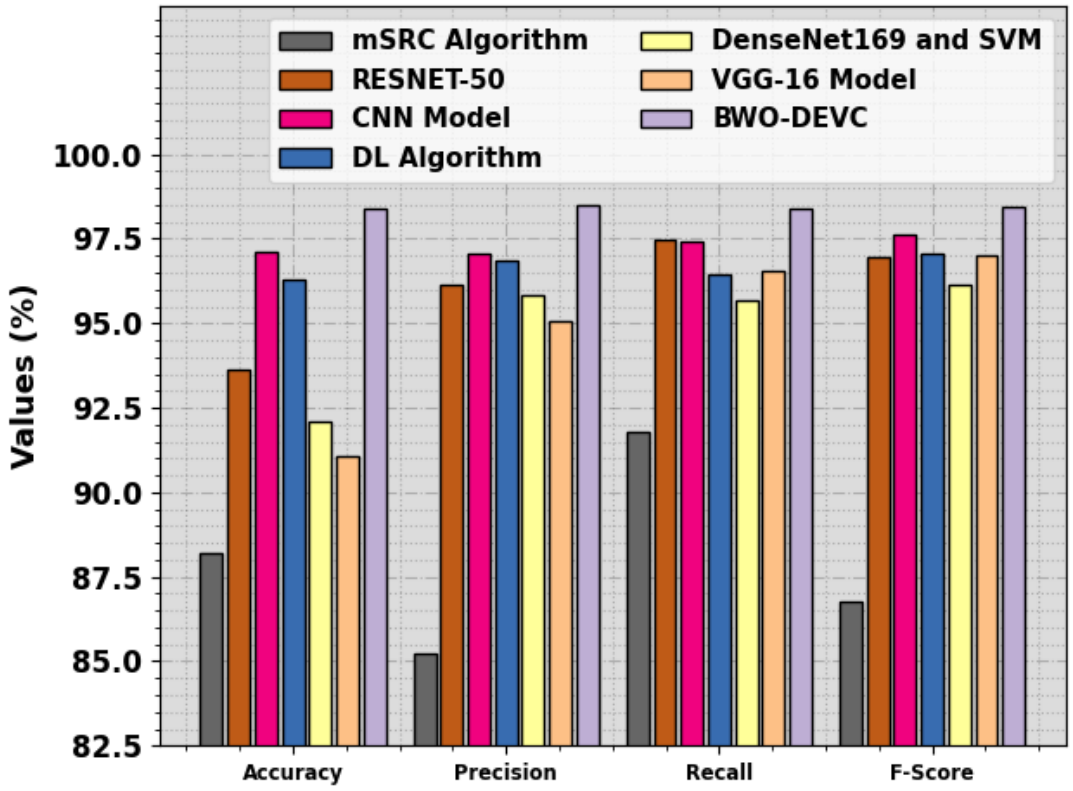

Fig. 12. Comparative outcome of BWO-DEVC approach with other systems

5. Conclusion

In this study, we have designed a new cloud assisted automatic CC detection and classification using the BWO-DEVC technique. The primary goal of BWO-DEVC method lies in the accurate recognition and classification of the CC on medical images in the cloud environment. It encompasses several subprocesses such as GF-based pre-processing, DarkNet-53 feature extractor, ensemble voting classification, and BWO-based hyperparameter tuning. For CC classification, the BWO-DEVC technique follows ensemble voting classifier comprising three DL algorithms such as GRU, BiLSTM, and LSTM. Finally, the hyperparameter selection of the DL approaches takes place using the BWO algorithm, which in turn enhances the CC detection results. An extensive set of experiments were made to validate the enhanced CC detection results of the BWO-DEVC algorithm. The extensive outcomes highlighted that the BWO-DEVC method reaches better performance than other techniques in the CC diagnostic process.

6. References

1. Agapito, G. and Cannataro, M., 2023. An Overview on the Challenges and Limitations Using Cloud Computing in Healthcare Corporations. Big Data and Cognitive Computing, 7(2), p.68.
2. Raju, A.S.N., Jayavel, K. and Rajalakshmi, T., 2022. An IoT-Enabled Healthcare System: Auto-predictive Colorectal Cancer with

Colonoscopy Images Combined with the Convolutional Neural Network. In High Performance Computing and Networking: Select Proceedings of CHSN 2021 (pp. 283-294). Singapore: Springer Singapore.
3. Kumar, D., Mandal, N. and Kumar, Y., 2023. Fog-based framework for diabetes prediction using hybrid ANFIS model in cloud environment. Personal and Ubiquitous Computing, 27(3), pp.909-916.
4. Xu, L., Walker, B., Liang, P.I., Tong, Y., Xu, C., Su, Y.C. and Karsan, A., 2020. Colorectal cancer detection based on deep learning. Journal of Pathology Informatics, 11.
5. Sirinukunwattana, K., Domingo, E., Richman, S.D., Redmond, K.L., Blake, A., Verrill, C., Leedham, S.J., Chatzipli, A., Hardy, C., Whalley, C.M. and Wu, C.H., 2021. Image-based consensus molecular subtype (imCMS) classification of colorectal cancer using deep learning. Gut, 70(3), pp.544-554.
6. Wang, K.S., Yu, G., Xu, C., Meng, X.H., Zhou, J., Zheng, C., Deng, Z., Shang, L., Liu, R., Su, S. and Zhou, X., 2021. Accurate diagnosis of colorectal cancer based on histopathology images using artificial intelligence. BMC medicine, 19(1), pp.1-12.
7. Korbar, B., Olofson, A.M., Miraflor, A.P., Nicka, C.M., Suriawinata, M.A., Torresani, L., Suriawinata, A.A. and Hassanpour, S., 2017. Deep learning for classification of colorectal polyps on whole-slide images. Journal of pathology informatics, 8.
8. Kather, J.N., Krisam, J., Charoentong, P., Luedde, T., Herpel, E., Weis, C.A., Gaiser, T., Marx, A., Valous, N.A., Ferber, D. and Jansen, L., 2019. Predicting survival from colorectal cancer histology slides using deep learning: A retrospective multicenter study. PLoS medicine, 16(1), p.e1002730.
9. Lee, S.H., Song, I.H. and Jang, H.J., 2021. Feasibility of deep learning-based fully automated classification of microsatellite instability in tissue slides of colorectal cancer. International Journal of Cancer, 149(3), pp.728-740.
10. Ho, C., Zhao, Z., Chen, X.F., Sauer, J., Saraf, S.A., Jialdasani, R., Taghipour, K., Sathe, A., Khor, L.Y., Lim, K.H. and Leow, W.Q., 2022. A promising deep learning-assistive algorithm for histopathological screening of colorectal cancer. Scientific Reports, 12(1), pp.1-9.
11. Sharma, P., Bora, K., Kasugai, K. and Balabantaray, B.K., 2020. Two Stage Classification with CNN for Colorectal Cancer Detection. Oncologie, 22(3).
12. Abdullah, S. and Ragab, M., 2023. Tunicate swarm algorithm with deep convolutional neural network-driven colorectal cancer classification from histopathological imaging data. Electronic Research Archive, 31(5), pp.2793-2812.
13. Zhou, P., Cao, Y., Li, M., Ma, Y., Chen, C., Gan, X., Wu, J., Lv, X. and Chen, C., 2022. HCCANet: histopathological image grading of colorectal cancer using CNN based on multichannel fusion attention mechanism. Scientific Reports, 12(1), p.15103.
14. Narasimha Raju, A.S., Jayavel, K. and Rajalakshmi, T., 2023, September. Histopathology exploratory evidence of discrepancy detection of carcinoma in the colorectal region using integrated CNN-GradCAM. In AIP Conference Proceedings (Vol. 2754, No. 1). AIP Publishing.
15. Hossain, M., Haque, S.S., Ahmed, H., Mahdi, H.A. and Aich, A.,

2022. Early stage detection and classification of colon cancer using deep learning and explainable AI on histopathological images (Doctoral dissertation, Brac University).
16. Singh, O. and Singh, K.K., 2023. An approach to classify lung and colon cancer of histopathology images using deep feature extraction and an ensemble method. International Journal of Information Technology, pp.1-12.
17. Lou, J., Xu, J., Zhang, Y., Sun, Y., Fang, A., Liu, J., Mur, L.A. and Ji, B., 2022. PPsNet: An improved deep learning model for microsatellite instability high prediction in colorectal cancer from whole slide images. Computer Methods and Programs in Biomedicine, 225, p.107095.
18. Basha, C.Z., Reddy, M.R.K., Nikhil, K.H.S., Venkatesh, P.S.M. and Asish, A.V., 2020, March. Enhanced computer aided bone fracture detection employing X-ray images by Harris Corner technique. In 2020 Fourth International Conference on Computing Methodologies and Communication (ICCMC) (pp. 991-995). IEEE.
19. Jabeen, K., Khan, M.A., Alhaisoni, M., Tariq, U., Zhang, Y.D., Hamza, A., Mickus, A. and Damaševičius, R., 2022. Breast cancer classification from ultrasound images using probability-based optimal deep learning feature fusion. Sensors, 22(3), p.807.
20. Roy, B., Malviya, L., Kumar, R., Mal, S., Kumar, A., Bhowmik, T. and Hu, J.W., 2023. Hybrid Deep Learning Approach for Stress Detection Using Decomposed EEG Signals. Diagnostics, 13(11), p.1936.
21. Xu, D. and Yin, J., 2023. An Improved Black Widow Optimization Algorithm for Engineering Constrained Optimization Problems. IEEE Access, 11, pp.32476-32495.
22. https://www.kaggle.com/datasets/andrewmvd/lung-and-colon-cancer-histopathological-images
23. Sakr, A.S., Soliman, N.F., Al-Gaashani, M.S., Pławiak, P., Ateya, A.A. and Hammad, M., 2022. An efficient deep learning approach for colon cancer detection. Applied Sciences, 12(17), p.8450.
24. AlGhamdi, R., Asar, T.O., Assiri, F.Y., Mansouri, R.A. and Ragab, M., 2023. Al-Biruni Earth Radius Optimization with Transfer Learning Based Histopathological Image Analysis for Lung and Colon Cancer Detection. Cancers, 15(13), p.3300.